Gas-liquid-solid flow modelling in a bubble column

G. M. Cartland Glover and S. C. Generalis*

School of Engineering and Applied Science, Division of Chemical Engineering and Applied

Chemistry, Aston University, Birmingham, B4 7ET U. K. Tel: +44 1213593611 ext 4707, Fax:

+44 1213594094

*Corresponding Author E-mail Address: S.C.Generalis@aston.ac.uk

Abstract

An alternative approach to the modelling of solid-liquid and gas-liquid-solid flows for a 5:1

height to width aspect ratio bubble column is presented here. A modified transport equation for

the volume fraction of a dispersed phase has been developed for the investigation of turbulent

buoyancy driven flows [1]. In this study, a modified transport equation has been employed for

discrete phase motion considering both solid-liquid and gas-liquid-solid flows. The modelling of

the three-phase flow in a bubble column was achieved in the case of injecting a slug of solid

particles into the column for 10 seconds at a velocity of 0.1 m s^{-1} and then the gas phase flow was

initiated with a superficial gas velocity of 0.02 cm s^{-1}.

Keywords: Two-Phase Flow, Three- Phase Flow, Bubble Columns, Computational Fluid

Dynamics, Mixture Models, Reynolds Stress Turbulence Transport.

Introduction

Understanding the complexity of the fluid dynamics in bubble column and airlift reactors is important due to their application in the chemical and bioprocess industries. Knowledge of the hydrodynamics of such reactors helps to determine the efficiency of biochemical production rates through transport processes such as inter-phase oxygen transfer, mixing of nutrients and reactants plus the effects that pH has on micro-organisms growth, metabolic pathways and cell lyses. For biochemical engineers the transport of a solid phase is important as the majority of bio-chemical reactions occur at a supported organism, or a flocculating microbe. It is important to understand the influence that the biomass has on the gas phase through inter-phase interactions and the impact that the biomass has on the liquid phase viscosity, because the fluid mixture can become a pseudo-plastic fluid as the culture grows and develops. Viscous broths also limit the effectiveness of the transport processes for each phase and the interfacial mass transfer of chemical [2-5].

Many parameters control the flow of solid and fluid phases through bubble column and airlift reactors, where the relative buoyancy of each discrete phase is the major driving force applied to the flow regime. Other factors that affect the complex flow phenomena include the coalescence and disruption of bubbles, surface tension, viscosity and pressure effects. The value of those parameters can influence the size, shape and volume fraction of the bubbly gas phase. Therefore, to improve the efficiency of multiphase reactors, the dynamic interactions between the discrete and continuous phases must be understood. The work that is presented here evaluates the aptness of mixture models implemented in the FLUENT code [6] to predict the motion of solid particles

in a bubbly flow (i.e. gas-liquid-solid mixture) to further the understanding of such complex reaction processes.

Earlier investigations into the transport of a bubbly gas phase in a liquid medium focused on the impact that the turbulence models employed have on the flow phenomena captured [1]. Part of the investigation included the development of an alternative mixture model where a diffusion term and a deviatoric stress tensor were included in the volume fraction equation for the gas phase that produced relevant profiles and flow fields [1]. This new alternative model can be employed in the implementation of a suspended solid phase. Solid phase transport in bubbly flows has been characterised through different numerical prediction methods [7-13]. Many models were implemented in the prediction of solid phase fractions, from a fluidised solid phase to suspended solids being agitated by discrete bubbles or by a pseudo-continuous gas phase [7-13]. It must be noted that neither of the solid phase schemes allow for particle collisions and interactions as described by Gidaspow [7-8] and Fan [10-11]. Due to these impositions, it was assumed that the solid phase fraction was small so that the influence of these effects is small and since the intention of the study was to model a fungal culture. Typically, fractions of 0.5% or 5 kg m^{-3} occur and therefore the influence of particle-particle interactions was assumed to be negligible [2-3].

Mathematical Models

Mixture Models

Earlier investigations into the transport of a bubbly gas phase in a liquid medium discuss the use of two mixture models [1]. The mixture models employed were based on the studies of Zuber and Findlay [14], Ishii et al. [15-16] and Manninen et al. [17] and are those examined in [1] (see Table 1 for the combinations of models employed for the specific cases). The only difference is the formulation of Ishii and Mishima's mixture viscosity [16], which is used in the scalar form of the mixture model presented in [1]. The relationship employed for the solid phase implementation of the mixture model is different, as μ^* is equal to 1. For the gas-liquid mixture model, μ^* took the form of a dimensionless ratio of the continuous and discrete phase viscosities. Also, note that particle interactions are ignored to reduce the model complexity (i.e. ignoring all bubble-bubble coalescence and breakup, bubble-solid collisions and solid-solid collisions).

Turbulence Transport Model

From previous investigations into the use of turbulence models when modelling buoyancy driven flows, it was determined that the Reynolds stress turbulence model provides the detail required to predict the turbulent interactions of the discrete phase with the continuous phase [1]. The exact Reynolds stress equation of turbulence transport was employed as a series of equations to enable closure of the unknown terms in the exact equation [1][18]. This includes the use of both the k-ε turbulence [19] transport equations plus the effects of buoyancy, pressure, strain and any rotation.

Model Application

Two meshed domains are employed to model solid-liquid and gas-liquid-solid flows that
correspond to the dimensional ratios used in the previous gas-liquid simulations [1]. The wall
conditions are applied to the left and right sides of the domain. A flow boundary inlet condition
was applied to 80% of the diameter of the column and was used as the gas phase inlet, with
conditions that include the volume fraction and the inlet velocity of the discrete phase modelled.
For full gas-liquid-solid flow, the top boundary condition was a pressure-inlet condition that
mimics the free surface of a liquid. When modelling the injection of the solid-liquid mixture for
either of the two or three phase flow representations, the mixture was injected through the central
10% of the top boundary condition. Conditions of velocity and volume fraction were applied to
this portion of the top boundary, though during this phase of the simulation the whole of the top
boundary was defined in terms of a velocity-inlet condition. Note that when solid phase was
injected into the domain the gas inlet boundary was defined as a wall condition, with the
assumption of no liquid loss through the base of the column.

The physical properties of the fluids simulated include the density, the particle size and the
viscosity of each phase. The respective densities for the gas, liquid and solid phases are 1.2
998.2 and 1080.2 kg m^{-3}. The gas and liquid viscosities are $1.8*10^{-5}$ and $1.0*10^{-3}$ kg m^{-1} s^{-1},
though the impact of the solid phase on the mixture viscosity is treated differently for the
different versions of the mixture model. The modified scalar equation form of the model
employs Ishii and Mishima's viscosity formulation [16], whereas the algebraic slip mixture

model requires the viscosity to be defined as 1 kg m^{-1} s^{-1} (this is caused by the definition of the mixture phase in the flow solver). The particle size of the discrete phase is an important parameter, defining the magnitude of the buoyancy driven forces applied to the liquid phase; for the air phase this was 5 mm and for the solid phase this was 0.1mm, where it was assumed that the form of both types of particle were spherical. The discretization techniques and under-relaxation factor applied when modelling discrete phase transport remain unchanged from the gas-liquid flow cases in [1] and this applies to both of the discrete phases modelled for reasons of consistency.

Solid-Liquid Flow

The aim of the solid-liquid flow test cases was to determine the effectiveness of either mixture model in capturing the motion of a suspended solid phase. The boundary conditions for the test cases were -0.1 m s^{-1} for the solid-liquid mixture velocity at the solid inlet (moving with the direction of gravity), where a solid phase fraction of 0.1 for both the SL1 and SL2 cases was taken (Table 1). The solid phase was injected for a period of 10 seconds at a time step of 0.1 seconds, consistent with earlier simulations [1]. This short injection period was followed by a further 190 seconds where the solid phase was allowed to drop to the base of the column.

Gas-Liquid-Solid Flow

Three cases were employed to cover three different combinations of the mixture models that describe gas-liquid-solid flow phenomena (see Table 1 for the specifications of the GLS1, GLS2 and GLS3 cases). During the first 10 s of the simulation, the solid phase was injected into the column through the solid inlet at a velocity of -0.1 m s^{-1} and solid phase fraction of 0.1 for both the scalar and algebraic slip mixture models [6][18] (a time-step size of 0.1 s was employed for each case [1]). This was similar to the solid-liquid simulations, except that 10 seconds after the solid phase injection was stopped, the gas phase injection starts. For comparison with the gas-liquid flow cases in [1] the vertical velocity for the gas phase was defined as a superficial gas velocity of 0.02 m s^{-1} with the phase fractions set to 0.6 as a scalar flux for GLS1 and GLS3, while the gas phase fraction for GLS2 was specified as 1. The full gas-liquid-solid simulations were then solved for a further 1800 steps or 180 seconds of flow time.

Results and Discussion

Comparison between experimental and simulated solid-liquid and gas-liquid-solid flow are difficult to achieve, as experimental data are provided on either velocity profiles [12], phase fraction profiles [8][13], [20] or contour plots [8-11][21-23]. It is apparent from [1] that the prediction of the gas phase fraction requires further refinement with the inclusion of coalescence and disruption models [24]. Consequently, we exploited the gas-liquid velocity profiles [1] to obtain a measure of the influence that the solid phase model has on the gas-liquid flow models. Therefore, to characterise the adequacy of multiphase flow models in capturing solid-liquid and

gas-liquid-solid motion in bubble columns time series, flow profiles and field plots are employed in a manner similar to [1].

Before evaluating the gas-liquid-solid flow models, the relevance of both the solid-liquid cases is examined in Figs. 1 - 3. Fig. 1 depicts the transport of the solid phase in the SL1 and SL2 simulations as a solids fraction time series, where both of the series are characterised by two sharp peaks at approximately 25 s and approximately 40 s of simulation time, after which there is a gradual reduction in the fraction for the next 60 seconds. These peaks arise when the first part of the injected slug of solid particles passes the halfway point and the gradual reduction in the fraction is due to solid particles entrained in the wake of the initial slug.

Time-averaged profiles (Fig. 2) of the solid-liquid mixture phase vertical velocities are parabolic and show that the bulk of the flow is down the centre of the column and upwards at the walls. It is noted that both curves are asymmetric, with high velocities observed for the SL2 case at the right wall and in the bulk of downward flow. The unsteady injection process causes the development and dissipation of wake structures that leads to the asymmetries observed in both velocity profiles. Fig. 3 illustrates the velocity vector fields and solid fraction contours at 40 s of simulated time for both solid-liquid flows. These plots capture the development of turbulent vortices caused by the introduction of the slug and detail how these vortices influence the discrete phase transport as the solid disperses through the liquid phase. Concentrating on the difference it is obvious that the transport of the solid for the SL1 case is faster than for the SL2, but as there are no comparisons with detailed experimentation, it is difficult to determine which of the two models is the most accurate. Despite this lack of verification, the effects predicted by the models

show plausible characteristics of solid motion through a liquid medium even with the significant differences observed in Fig. 1 and Fig. 3.

The time series of the solids fraction for the GLS1, GLS2 and GLS3 cases in Fig. 4 show a similar increase (c.f. Fig. 1) in the solids fraction between 25 and 40 seconds of simulation time. The influence of the oscillating flow field generated by the gas phase motion was also observed in these series as the solids fraction fluctuated about an average value (except for the GLS1 simulation where the fraction gradually reduces with time). Note that there is a difference in the form of the GLS2 and GLS3 time-series, where the fluctuation in the hold-up is regular for the GLS2 series and is irregular for the GLS3 curve. This change in form is a result of the different solid phase representations employed (Table 1).

The profile plots in Fig. 5 portray the time-averaged vertical mixture velocity for the scalar equation form of the mixture model (from [1]) and for the GLS1, GLS2 and GLS3 cases. We note that the GLS1 and GLS2 cases are asymmetric while the GLS3 cases is symmetric with respect to the column centreline. Comparing the profile for the GLS3 case and the gas-liquid flow of [1], the profiles are similar, except that the GLS3 profile is 0.02 - 0.03 m s^{-1} less than the gas-liquid simulation of [1]. The corresponding profiles for the gas phase hold-up (Fig. 6) also highlights the similarities between the gas-liquid flow [1] and GLS3 cases with a difference of 2%. Note that GLS1 profile is asymmetric and GLS2 curve has a parabolic profile with a flattened peak.

Fig. 7 depicts the volume fraction of the solid phase for all the solid-liquid and gas-liquid- solid cases. The SL1 and SL2 curves differ, with the fraction predicted by the SL1 model slightly

greater than the SL2 case. The SL1 profile has two distinct regions corresponding to the wall and

central sections of the domain where a constant increase in the fraction to the central section

occurs. At this point the fraction becomes constant. The SL2 profile is flatter and similar in form

to the gas fraction profiles except that the asymmetries observed in the velocity profile (Fig. 2)

are also present with a bias to the left. The GLS1 case has a flat profile across the column at a

very low solids fraction of 0.1 %. The solids fraction profiles for the GLS2 and GLS3 cases

display a plug flow form with fractions in the range of 1 to 2 %.

Field plots of velocity vectors and the phase fraction contours of each discrete phase for the

GLS1, GLS2 and GLS3 cases at 100 seconds of flow time are found in Figs. 8 - 10. The vector

field plots for cases GLS1 to GLS3 in Figs. 8A - 10A are similar to the flow fields solved by the

equivalent gas-liquid flow models of [1] and shows that the introduction of a solid phase

transport model does not disrupt the flow of the gas phase through a bubble column. This is

confirmed by the contours of the gas fraction, which also correspond to the structures depicted by

the gas-liquid flow models in [1].

The solids fraction contours for all the three-phase models are different in structure and again are

dependent on the volume fraction equation used. This determines how the velocity field for the

liquid phase develops, as observed in the profile plots (Figs. 5 - 7). The GLS2 solids fraction

contours as depicted in Fig. 9C show that the flow structure has an appreciable effect on the solid

phase transport. By comparing the gas and solids fractions, we observe that the gas phase

influences the location or regions where solid phase tends to congregate (i.e. a region where the

gas fraction is low corresponds to regions where high solid phase fractions occur and vice versa).

The three-phase model that employed the scalar mixture model for both of the discrete phases (GLS3), displayed the greater relevance to reality by showing consistency with the earlier gas-liquid simulations and the experimental investigations of Warsito [20]. However, further work is required to improve the models employed and this would include extending the transport equations to three-dimensional flow and the thorough comparison of the three-phase models with experimental data. Modifications to the multiphase models would include effects such as the coalescence and dispersion of bubbles, particle wake and wall interactions plus the influence of particle-particle interactions [7-8][10-11]. The use of an energy balance equation would determine the impact of internal energy on fluid flow derived from the motion of bubbles and solid particles, particularly when collisions occur [6].

Acknowledgements

Nomenclature

k   = kinetic energy ($m^2 \, s^{-2}$)

ε = rate of dissipation of turbulent energy ($m^2 \, s^{-2}$)

μ^* = viscosity power function, different for gas (~0.4) and solid (1) phases

References

[1] Cartland Glover, G. M., Generalis, S. C. The modelling of buoyancy driven flow in bubble columns (Submitted to in Chemical Engineering and Processing)

[2] Bailey, J. E. and Ollis, D. F., Biochemical Engineering Fundamentals, McGraw-Hill, 1986, London, England

[3] Chisti, M. Y., Airlift Bioreactors, Elsevier Science Publishers Ltd, 1989, London, England

[4] Deckwer, W. -D., Bubble Column Reactors, Jon Wiley and Sons Ltd, Chichester, England, 1992

[5] Joshi, J. B. Computational flow modelling and design of bubble column reactors, Chem. Eng. Sci. 56(20-21) (2001) 5893-5933

[6] Fluent, Fluent Europe Ltd, Sheffield Airport Business Park, Europa Link, Sheffield S9 1XU (www.fluent.com)

[7] Ding, J. and Gidaspow, D. A bubbling fluidization model using kinetic theory of granular flow, AICHE J. 36 (1990) 523-538

[8] Wu, Y. X. and Gidaspow, D. Hydrodynamic simulation of methanol synthesis in gas-liquid slurry bubble column reactors, Chem. Eng. Sci. 55(3) (2000) 573-587

[9] Padial, N. T., Vander Heyden, W. B., Rauenzahn, R. M. and Yarbro, S. L. Three-dimensional simulation of a three-phase draft-tube bubble column, Chem. Eng. Sci. 55(16) (2000) 3261-3273

[10] Li, Y., Yang, G. Q., Zhang, J. P. and Fan, L. S. Numerical studies of bubble formation dynamics in gas-liquid-solid fluidization at high pressure, Powder Tech. 116(2-3) (2001) 246-260

[11] Michele, V., Dziallas, H. Enss, J. and Hempel, D. C. Three-phase flow in bubble columns – measurement and modelling, Proceedings of the Third European Congress in Chemical Engineering 26-28 June 2001

[12] Mitra-Majumdar, D., Farouk, B., Shah, Y. T., Macken, N., and Oh, Y. K. Two- and three-phase flows in bubble columns: numerical predictions and measurements, Ind. Eng. Chem. Res. 37 (1998) 2284-2292

[13] Zuber, N. and Findlay, J. A. Average volumetric concentrations in two-phase flow systems, J. of Heat Transfer 87 (1965) 453-468

[14] Ishii, M. and Zuber, N. Drag coefficient and relative velocity in bubbly, droplet and particulate flow, AIChE J. 25(5) (1979) 843-854

[15] Ishii, M. and Mishima, K. Two-fluid model and hydrodynamic constitutive relations, Nuclear Eng. and Des. 82 (1984) 107-126

[16] Manninen, M. Taivassalo V. and Kallio, S. On the mixture model for multiphase flow, VTT Publications 288 (1996) IBSN 951-38-4946-5

[17] FLUENT 5 Users Guide, Fluent Incorporated, Centerra Park, 10 Cavendish Court, Lebanon, NH03766, USA, 1998

[18] Launder, B. E. and Spalding, D. B., The numerical computation of turbulent flows, Computer Methods in Applied Mechanics and Engineering, 3 (1974) 269-289

[19] Warsito, Ohkawa, M., Maezawa, A. and Uchida, S. Flow structure and phase distributions in a slurry bubble column, Chem. Eng. Sci. 52 (21-22) (1997) 3941-3947

[20] Warsito, Ohkawa, M., Kawata, N. and Uchida, S. Cross-sectional distributions of gas and solid holdups in slurry bubble column investigated by ultrasonic computed tomography, Chem. Eng. Sci. 54(21) (1999) 4711-4728

[21] Warsito, W. and Fan, L.-S. Measurement of real-time flow structures in gas-liquid and Gas-liquid-solid flow systems using electrical capacitance tomography (ECT), Chem. Eng. Sci. 56(21-22) (2001) 6455 –6462

[22] Utomo, M. B., Warsito, W., Sakai, T. and Uchida S. Analysis of distributions of gas and TiO_2 particles in slurry bubble column using ultrasonic computed tomography, Chem. Eng. Sci. 56(21-22) (2001) 6073 –6079

[23] Prince, M. J. and Blanch, H. W. Bubble coalescence and break-up in air-sparged bubble columns AIChE J. 36(10) (1990) 1485-1499

Figures and Tables

Fig. 1. Times series of the solid phase volume fraction (-) at a height of 0.5 m from the base of the column on the column centreline for the simulations involving the solid-liquid simulations; SL1: ▬; SL2: ┈;

Fig. 2. Profile across the width of the column of the time-averaged vertical mixture phase velocity (m s^{-1}) at a height of 0.5 m from the base of the column involving the solid-liquid simulations; SL1: ⊟; SL2: ◇;

Fig. 3. SL1 and SL2 field plots at 40 seconds where the velocity vectors scale is from 0 m s^{-1} for small vectors to 0.1 m s^{-1} for large vectors and the solid fraction contour scale is from 0 for black contours to 0.05 for light grey contours; A: SL1 velocity vectors; B: SL1 solid fraction contours; C: SL2 velocity vectors; D: SL2 solid fraction contours;

Fig. 4. Times series of the solid phase volume fraction (-) at a height of 0.5 m from the base of the column on the column centreline for the simulations involving the gas-liquid-solid simulations; GLS1: ——; GLS2: ----; GLS3: ·······;

Fig. 5. Profile of the time-averaged vertical mixture phase velocity (m s^{-1}) across the width of the column at a height of 0.5 m from the base of the column involving the gas-liquid and gas-liquid-solid simulations; GL2: -•-; GLS1: △; GLS2: ⊖; GLS3: ✕;

Fig. 6. Profile of the time-averaged gas phase volume fraction (-) across the width of the column at a height of 0.5 m from the base of the column involving gas-liquid and gas-liquid-solid simulations; GL2: -•-; GLS1: △; GLS2: ⊖; GLS3: ✕;

Fig. 7. Profile of the time-averaged solid phase volume fraction (-) across the width of the column at a height of 0.5 m from the base of the column involving the solid-liquid and gas-liquid-solid simulations; SL1: ⊟; SL2: ◇; GLS1: △; GLS2: ⊖; GLS3: ✕;

Fig. 8. GLS1 field plots at 100 seconds; A: Vectors of mixture velocity magnitude (m s^{-1}) for the 5:1 two-dimensional plane mesh; Scale is from 0 (small black vectors) to 0.5 m s^{-1} (large light grey vectors); B: Contours of gas phase volume fraction (-) for the 5:1 two-dimensional plane mesh; Scale is from 0 (black) to 0.25 (light grey); C: Contours of solid phase volume fraction (-) for the 5:1 two-dimensional plane mesh; Scale is from 0 (black) to 0.001 (light grey);

Fig. 9. GLS2 field plots at 100 seconds; A: Vectors of mixture velocity magnitude (m s^{-1}) for the 5:1 two-dimensional plane mesh; Scale is from 0 (small black vectors) to 0.9 m s^{-1} (large light grey vectors); B: Contours of gas phase volume fraction (-) for the 5:1 two-dimensional plane mesh; Scale is from 0 (black) to 0.15 (light grey); C: Contours of solid phase volume fraction (-) for the 5:1 two-dimensional plane mesh; Scale is from 0 (black) to 0.05 (light grey);

Fig. 10. GLS3 field plots at 100 seconds; A: Vectors of mixture velocity magnitude (m s^{-1}) for the 5:1 two-dimensional plane mesh; Scale is from 0 (small black vectors) to 0.5 m s^{-1} (large light grey vectors); B: Contours of gas phase volume fraction (-) for the 5:1 two-dimensional plane mesh; Scale is from 0 (black) to 0.5 (light grey); C: Contours of solid phase volume fraction (-) for the 5:1 two-dimensional plane mesh; Scale is from 0 (black) to 0.05 (light grey);

Table 1 Application of the mixture model to two and three-phase flows, where the velocity is an inlet condition through either the top or bottom surfaces.
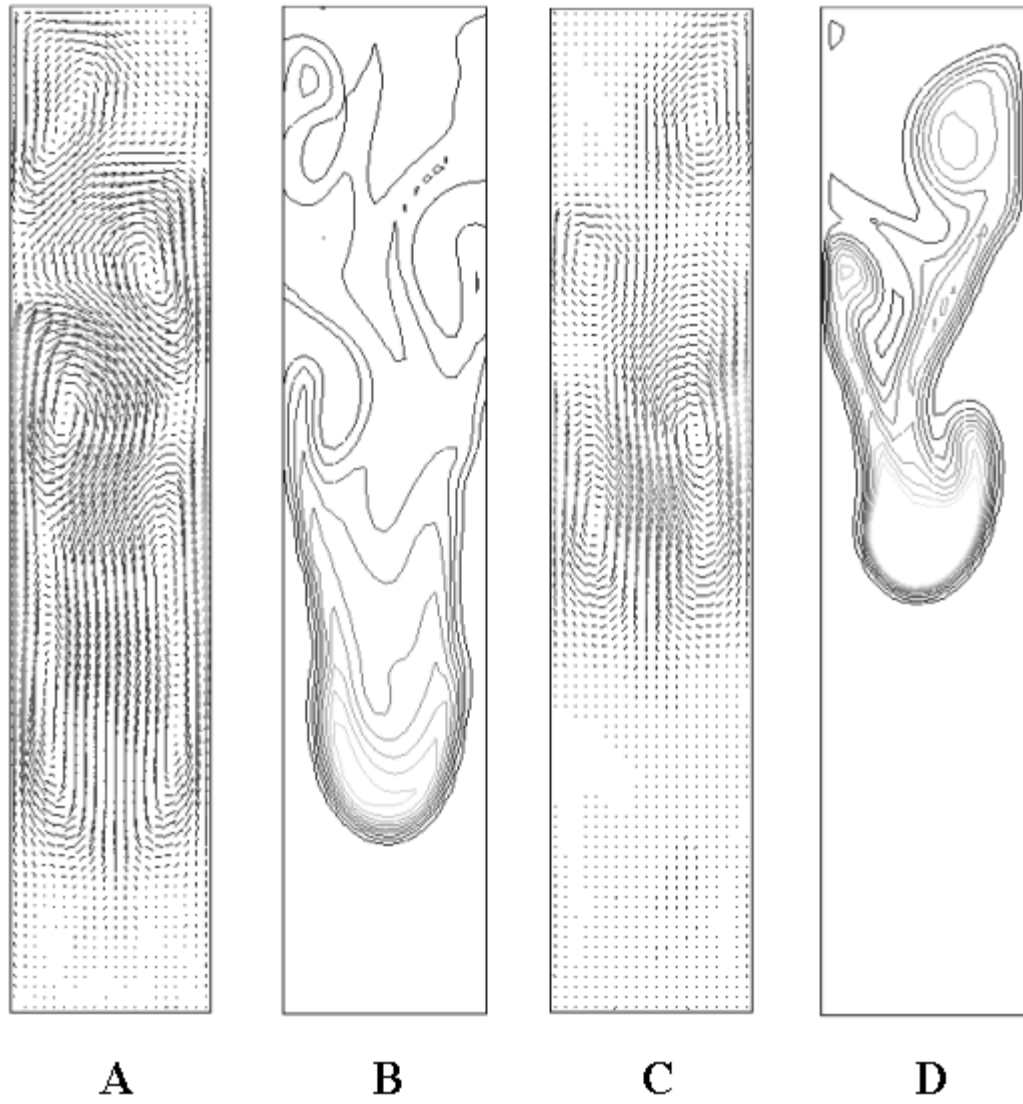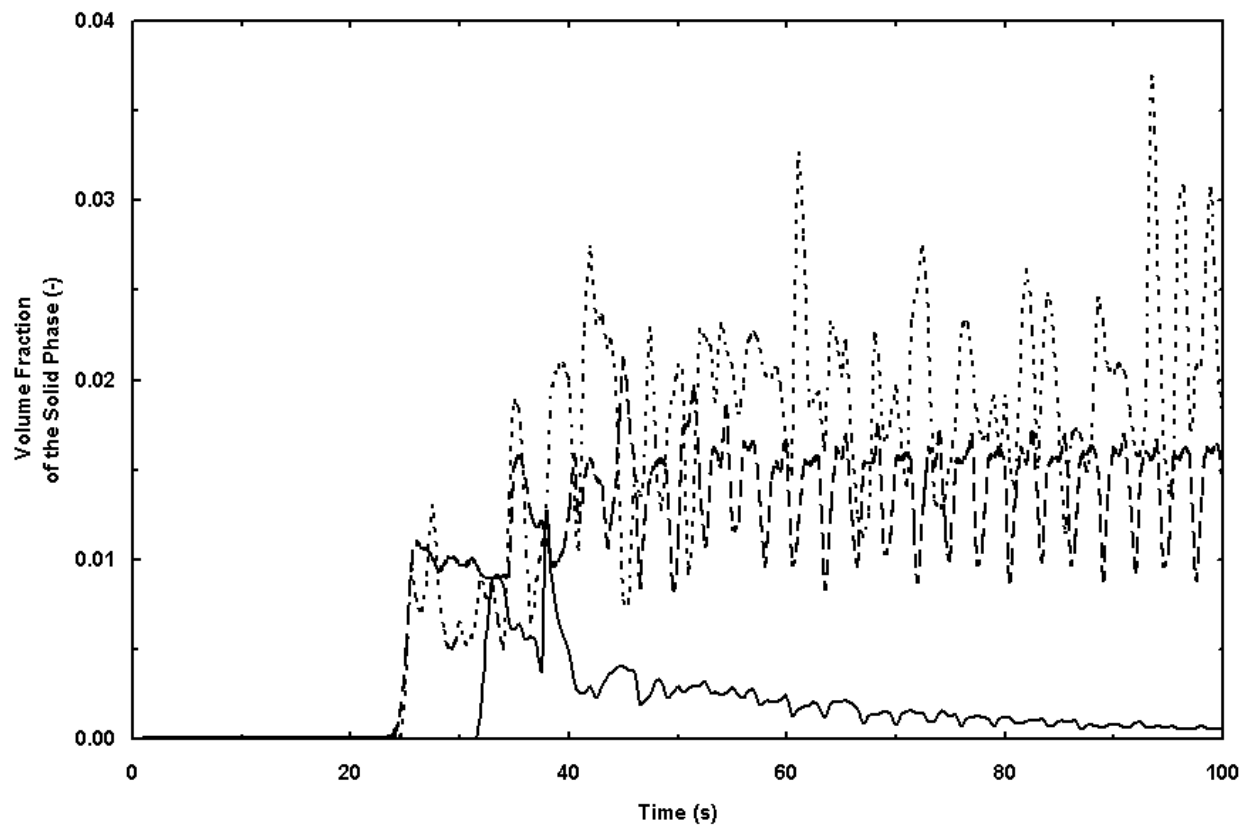
Fig. 1.

Fig. 2.

A **B** **C** **D**
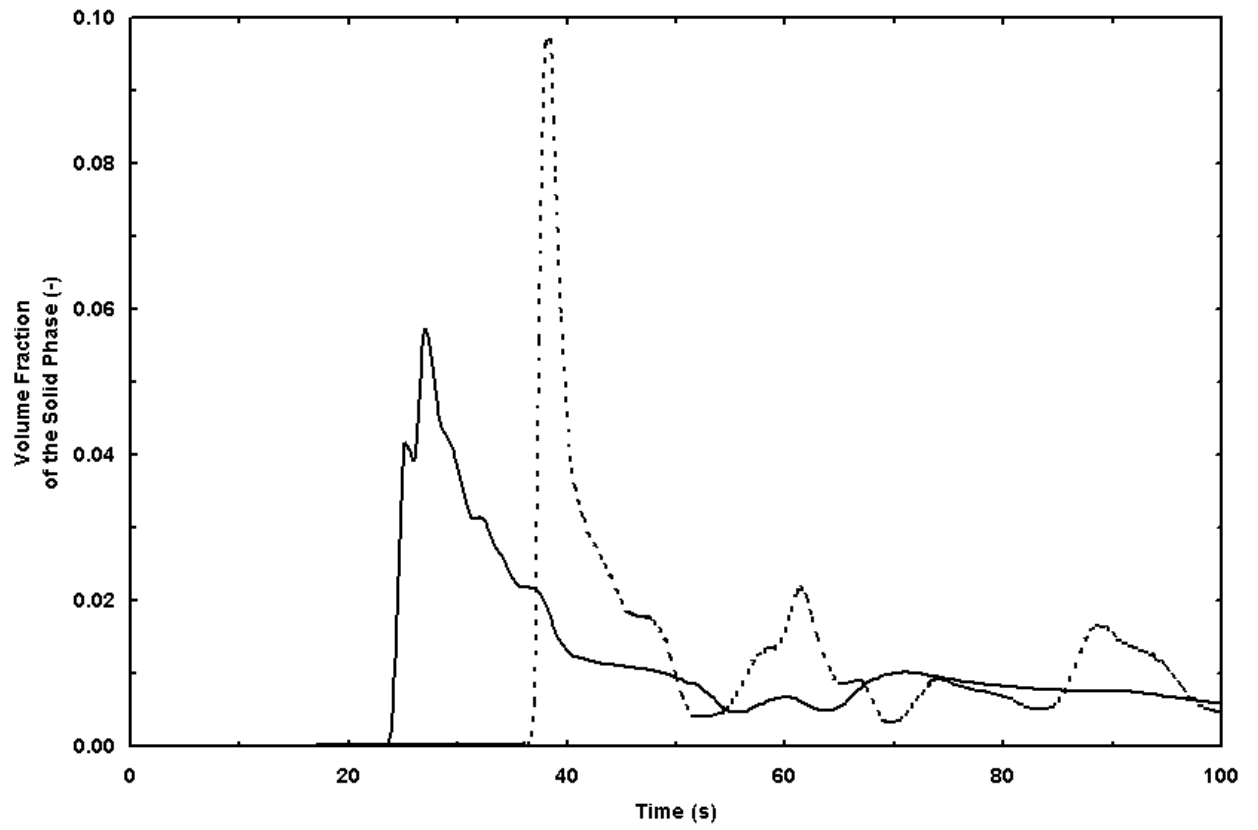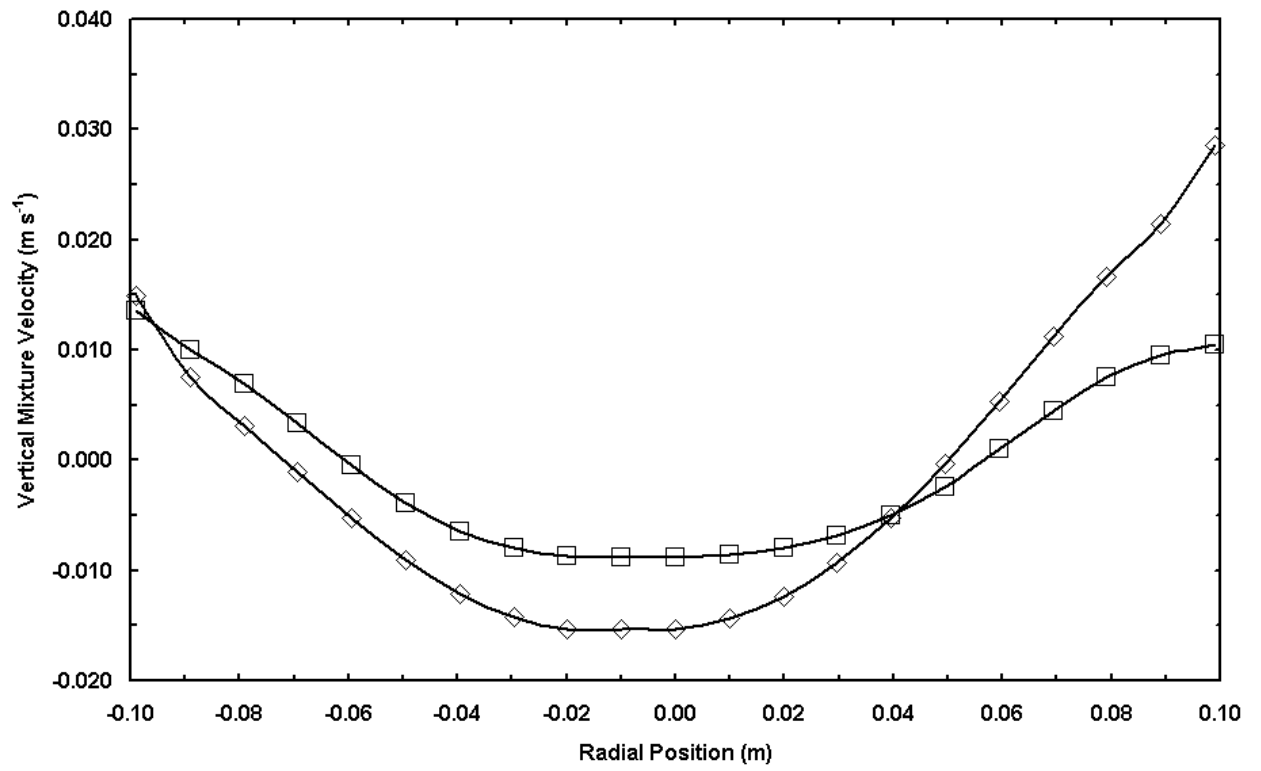
Fig. 3.

Fig. 4.

Fig. 5.

Fig. 6.

Fig. 7.

A   **B**   **C**

Fig. 8.

A   **B**   **C**

Fig. 9.

A   **B**   **C**
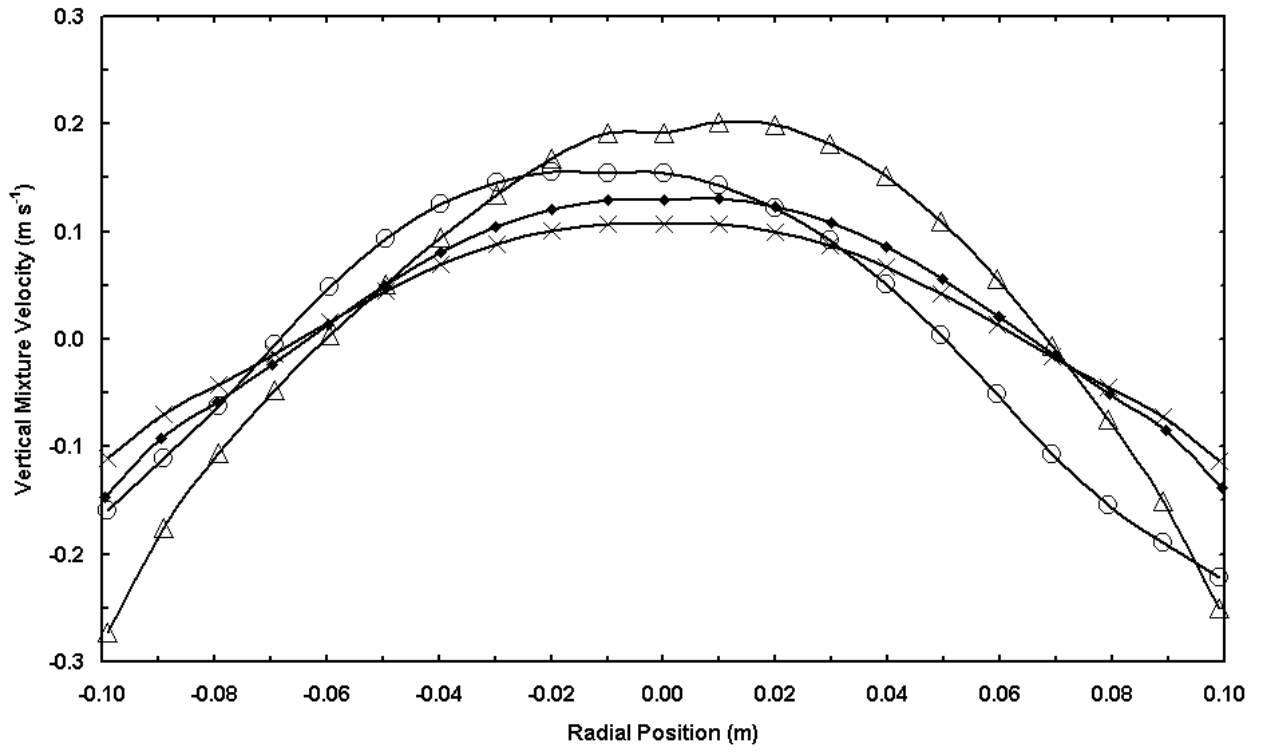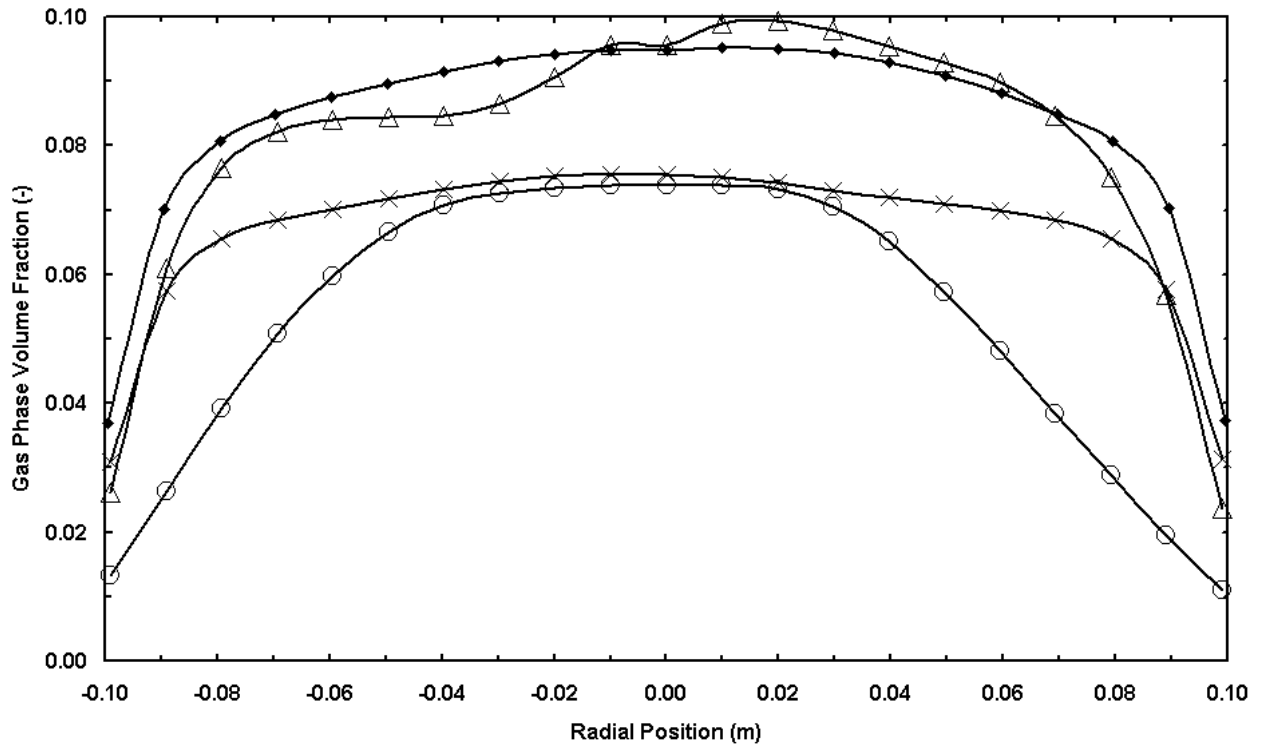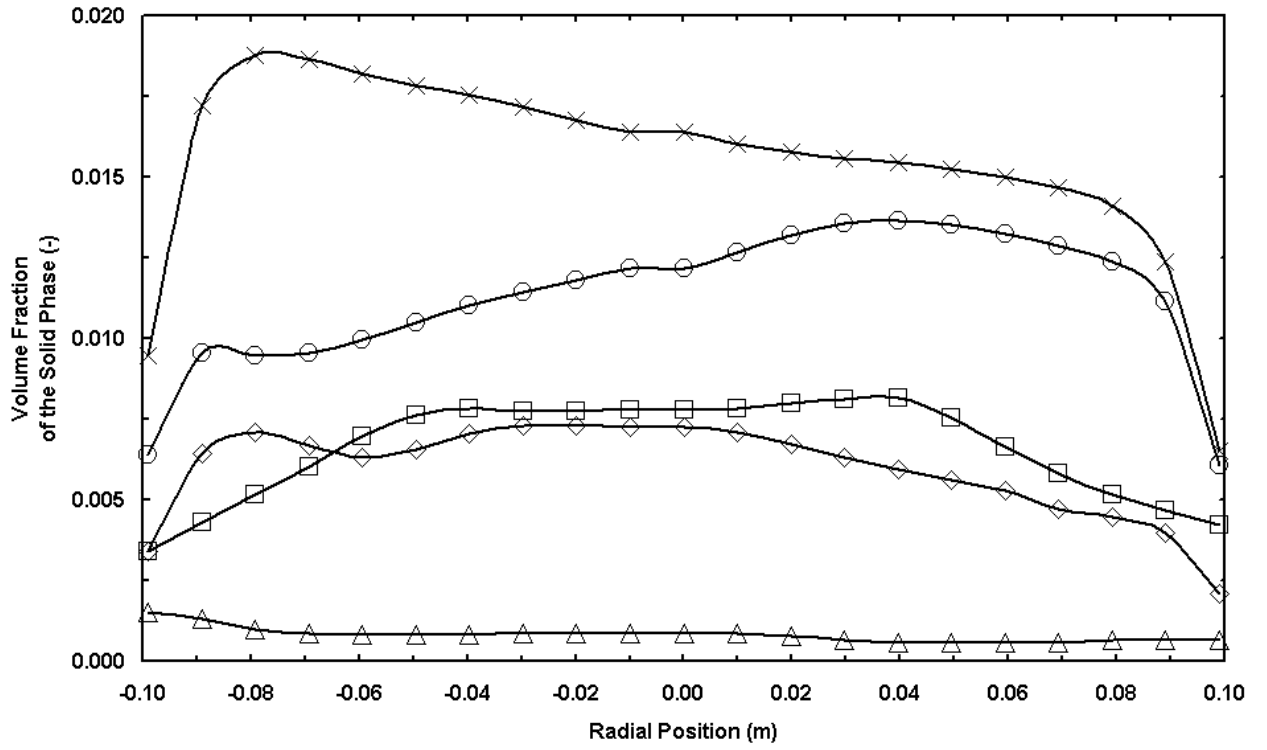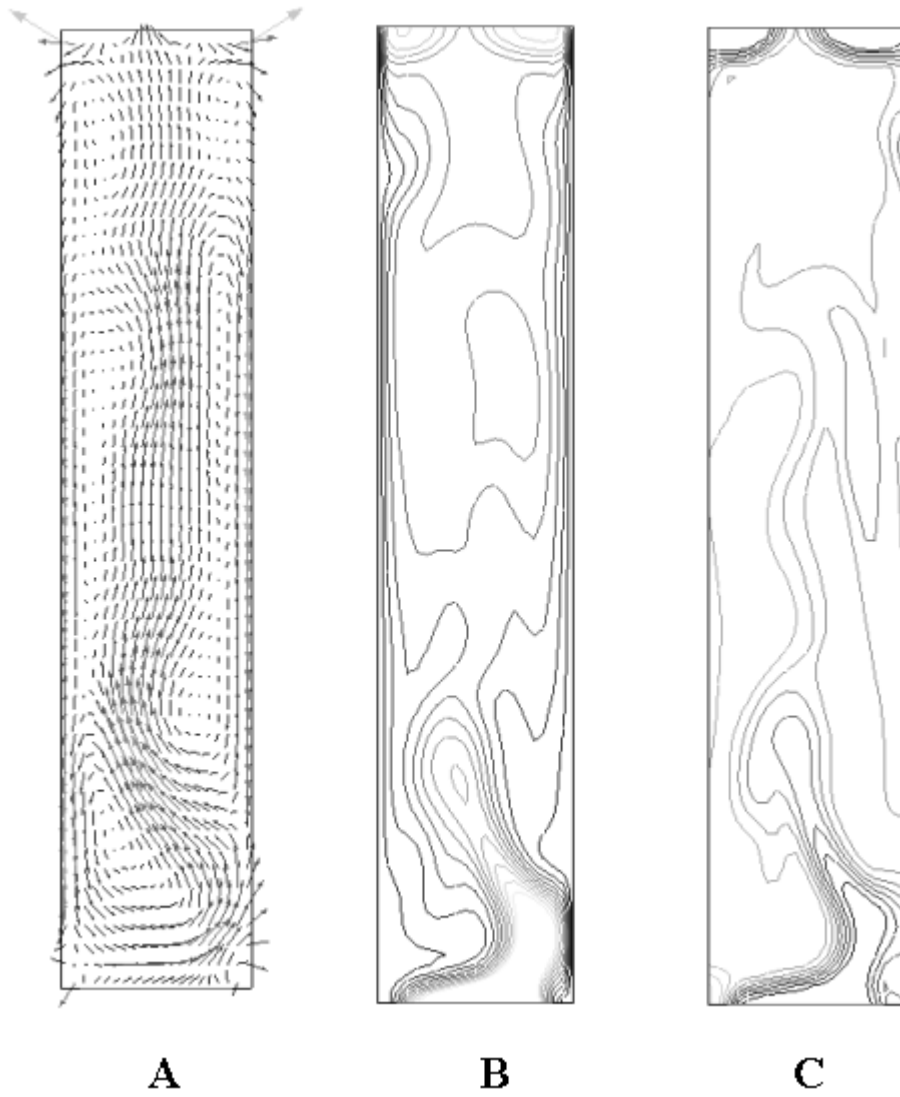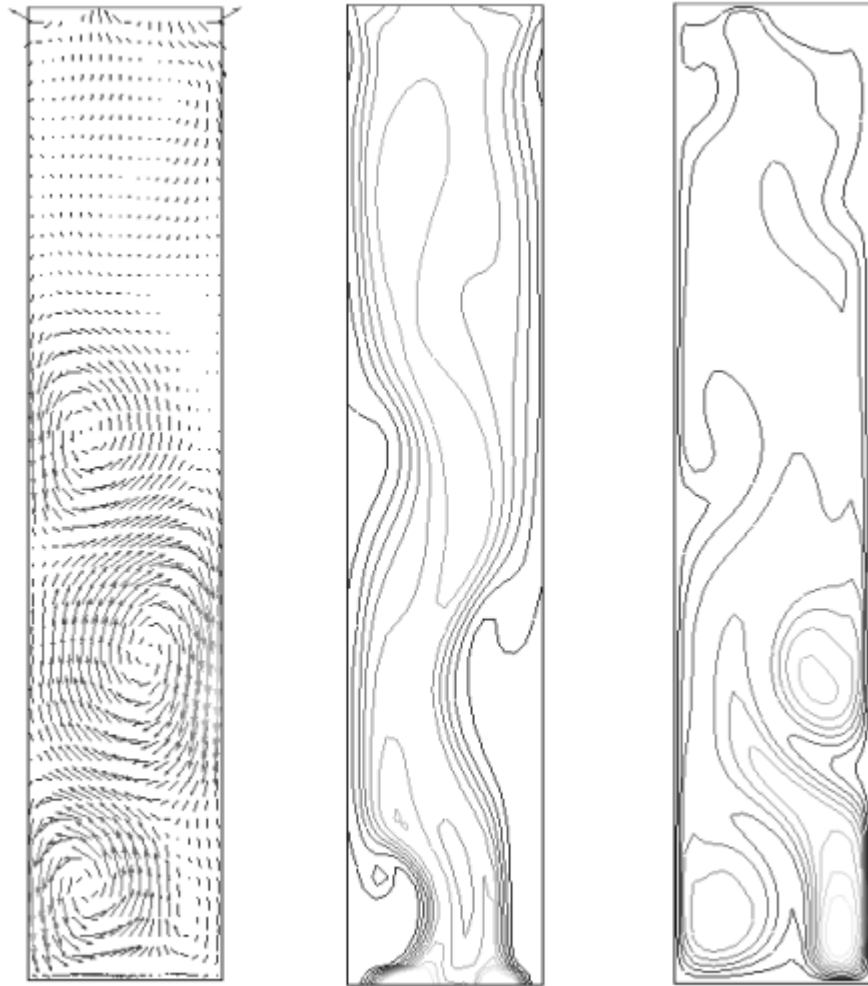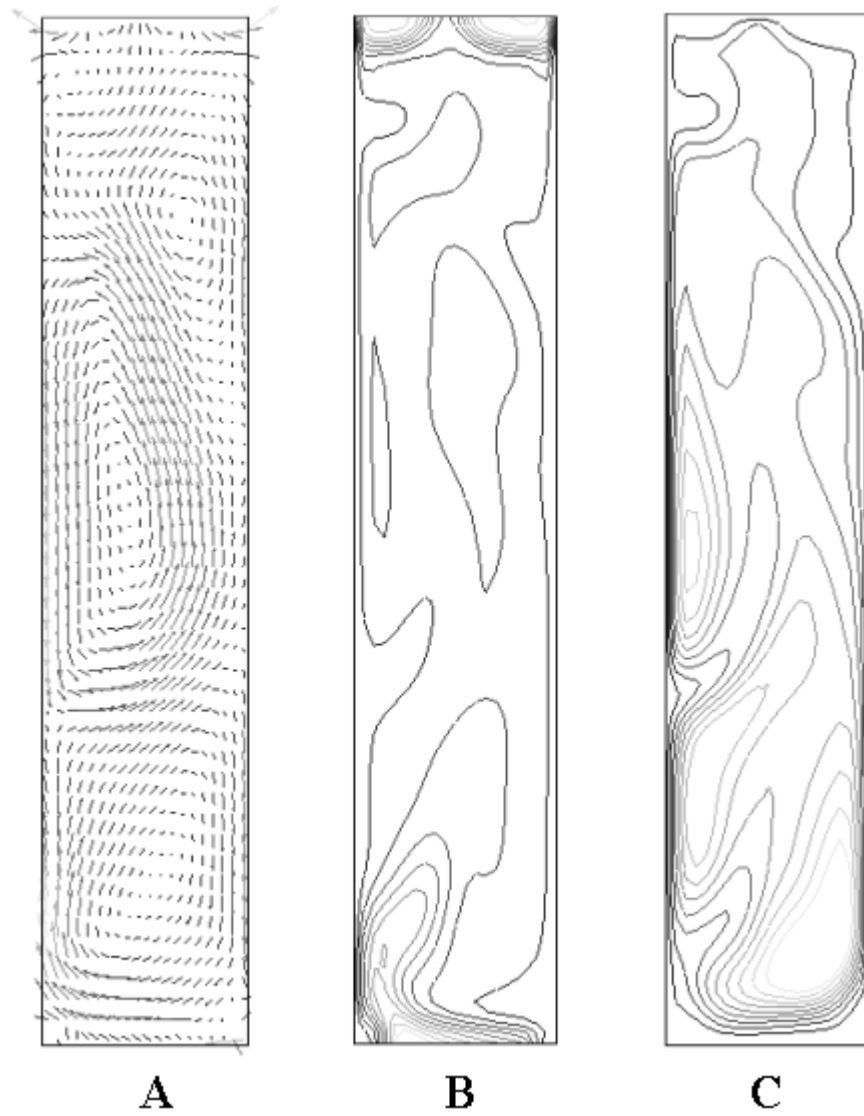
Fig. 10.

Table 1

Case	Number of Discrete Phases	Gas Phase				Solid Phase				Turbulence Model
		Mixture Model	Velocity (m s^{-1})	Definition	Value	Mixture Model	Velocity (m s^{-1})	Definition	Value	
GL1 [1]	1	Algebraic Slip	0.032	Fraction	1	-	-	-	-	Reynolds Stresses Model
GL2 [1]	1	Modified Scalar Equation	0.032	Flux	0.6	-	-	-	-	Reynolds Stresses Model
SL1	1	-	-	-	-	Algebraic Slip	0.1	Fraction	0.1	Reynolds Stresses Model
SL2	1	-	-	-	-	Modified Scalar Equation	0.1	Flux	0.1	Reynolds Stresses Model
GLS1	2	Modified Scalar Equation	0.032	Flux	0.6	Algebraic Slip	0.1	Fraction	0.1	Reynolds Stresses Model
GLS2	2	Algebraic Slip	0.032	Fraction	1	Modified Scalar Equation	0.1	Flux	0.1	Reynolds Stresses Model
GLS3	2	Modified Scalar Equation	0.032	Flux	0.6	Modified Scalar Equation	0.1	Flux	0.1	Reynolds Stresses Model